

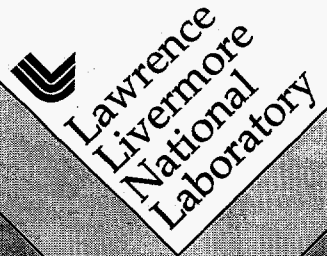
CONF. 960543--6

Thomson Scattering Stray Light Reduction Techniques Using a CCD Camera

D.G. Nilson, D.N. Hill, J.C. Evans, T.N. Carlstrom, C.L. Hsieh, R.E. Stockdale

This paper was prepared for submittal to the
11th Topical Conference on High-Temperature Plasma Diagnostics
Monterey, CA
May 12-16, 1996

February 1996



This is a preprint of a paper intended for publication in a journal or proceedings. Since changes may be made before publication, this preprint is made available with the understanding that it will not be cited or reproduced without the permission of the author.

DISCLAIMER

This document was prepared as an account of work sponsored by an agency of the United States Government. Neither the United States Government nor the University of California nor any of their employees, makes any warranty, express or implied, or assumes any legal liability or responsibility for the accuracy, completeness, or usefulness of any information, apparatus, product, or process disclosed, or represents that its use would not infringe privately owned rights. Reference herein to any specific commercial product, process, or service by trade name, trademark, manufacturer, or otherwise, does not necessarily constitute or imply its endorsement, recommendation, or favoring by the United States Government or the University of California. The views and opinions of authors expressed herein do not necessarily state or reflect those of the United States Government or the University of California, and shall not be used for advertising or product endorsement purposes.

REF ID: A61111

Thomson Scattering Stray Light Reduction Techniques Using a CCD Camera

D.G. Nilson,^{a)} D.N. Hill, J. C. Evans

Lawrence Livermore National Laboratory, Livermore, California

T.N. Carlstrom, C.L. Hsieh, R.E. Stockdale

General Atomics, P.O. Box 85608, San Diego, California 92186-9784

The DIII-D Thomson scattering system has been expanded to measure divertor plasma temperatures from 1–500 eV and densities from 0.05 to $8 \times 10^{20} \text{m}^{-3}$. To complete this system, a difficult stray light problem was overcome to allow for an accurate Rayleigh scattering density calibration. The initial stray light levels were over 500 times higher than the expected Rayleigh scattered signal. Using a CCD camera, various portions of the vessel interior were examined while the laser was fired through the vessel in air at atmospheric pressure. Image relaying, exit window tilting, entrance and exit baffle modifications, and a beam polarizer were then used to reduce the stray light to acceptable levels. The CCD camera gave prompt feedback on the effectiveness of each modification, without the need to re-establish vacuum conditions required when using the normal avalanche photodiode detectors (APD). Once the stray light was sufficiently reduced, the APD detectors provided the signal time history to more accurately identify the source location. We have also found that certain types of high reflectance dielectric

coatings produce 10 to 15 times more scatter than other types of more conventional coatings. By using low-scatter mirror coatings and these new stray light reduction techniques, we now have more flexibility in the design of complex Thomson scattering configurations required to probe the central core and the new radiative divertor regions of the DIII-D vessel.

INTRODUCTION

To make accurate plasma density measurements, the new divertor Thomson scattering system on DIII-D requires a calibration using a known scattering medium. Raman scattering in 100–200 Torr of hydrogen or Rayleigh scattering in several Torr of argon or nitrogen provides the proper signal level to calibrate the APD based detector system. The safety issues that arise from this pressure of hydrogen, combined with the excessive stray light generated from suspended dust at pressures above 10 Torr prohibit the Raman scattering method. Using Rayleigh scattering, we select argon over nitrogen due to its larger scattering cross-section and its lower adsorption rate on the vessel walls. However, given that the Rayleigh scattered wavelength is very close to that of the laser, and the APD detectors saturate at very low levels, the stray laser light must be minimized. This requires careful beam transport design and alignment to eliminate major stray light generators.

The existing core Thomson scattering system has required a low stray light level since it is calibrated with argon gas as well. However, two significant geometry differences make stray light reduction much more difficult on the divertor Thomson system. First, razor blade light traps used extensively in the viewing region of the core Thomson system could not be used because they would be located on the vessel floor, directly beneath the plasma strike point. This floor perturbation could possibly alter the local recycling in this region, as well as lead to tile failure due to the excessive heat loads on adjacent tiles. Secondly, the divertor Thomson scattering viewing region is located directly below the exit window, which is expected to be a major source of stray light. These differences did in fact cause severe stray light problems, which lead to

the development of new techniques used to identify the stray light sources and the reconfiguration of hardware to reduce them.

I INITIAL SYSTEM DESIGN

The divertor Thomson system uses a multi-pulse, 1.06 μm laser to probe the divertor region of the DIII-D vessel. This Nd:YAG laser (1 Joule, 20 Hz) originates from the existing core Thomson scattering system and is diverted onto an extended optical bench located directly below the vessel (Fig. 1).¹⁻³ A 5.6 M lens focuses this 20 mm diameter beam to a 1.3 mm diameter spot located 11 cm above the vessel floor. Two COHU CCD cameras (Model 4812) are placed behind the beam steering mirrors beneath the vessel to monitor the beam alignment. Output from these cameras is monitored by a beam analyzer which provides energy line profiles and beam positioning information. A glass beam splitter placed between the two cameras directs a small portion of the beam into a calibrated integrating sphere to monitor the total beam energy. To reduce stray light generated by these optical elements, an array of twelve double edged baffle cones are placed between the vacuum window and the vessel floor (Fig. 1) A similar array consisting of seven baffles is positioned between the ceiling and exit window to reduce possible reflections from the exit window. The array apertures provide a 3 mm radial clearance from the laser as it enters and exits the vessel. We achieve additional stray light reduction using an exit vacuum window tilted at Brewster's angle. Beyond this window, a small fraction of the beam is split off to another alignment monitor camera, while the main beam enters a dump constructed of NG-4 absorbing glass. Two floor

tiles are scalloped 3 mm deep and placed in the region behind the laser scattering volume to provide a modest viewing dump. This reduces the background radiation for plasmas whose incident field line angle with the vessel floor is less than 1.3° , which includes most plasmas of interest. A more complete description of the overall system including the detection and analysis techniques is given in a companion paper at this conference.⁴

II. SYSTEM ALIGNMENT

Low stray light levels require good overall system alignment and ample clearances for the laser beam through the transport hardware. A 3 mm radial clearance was initially provided between the laser and the entrance and exit baffle arrays. To ensure the laser is well centered in these baffles, a careful alignment procedure was followed. First, each end of the two baffle tube arrays was aligned to a HeNe laser. Prior to the initial plasma operations, the Thomson scattering laser is made colinear with this HeNe laser as well. Two $1.06 \mu\text{m}$ LED's were then centered on this HeNe laser at each end of the viewing region near the vessel floor. These LEDs provided fiducials for the initial alignment of two linear fiber optic arrays located at each end of the image plane. Before initial plasma operations, the LEDs were removed, and the fiber arrays then collected scattered laser light. This gave an absolute *in-situ* measurement of the laser tangential position to within $\pm 130 \mu\text{m}$, thus ensuring the laser was well centered toroidally in the baffle arrays.

III. USE OF CCD CAMERA

During initial Rayleigh scattering calibration attempts, the stray laser light was found to be several orders of magnitude above the acceptable level of 1.3×10^4 photons/channel, as measured at the entrance to the collection optics located on the vessel wall. Corresponding signal timing information showed that the stray light reached the collection optics 15–30 ns after the scattered signal, indicating that it was being generated from the vessel ceiling region rather than near the floor. Attempts to reduce the stray light by decreasing the input laser beam diameter and repositioning the focus lens along the beam path to achieve a better transmission through the baffle arrays had no measurable effect. With the vessel vented to the atmosphere, a CCD camera (COHU, Model 4812) was positioned on the vessel floor to observe any possible stray light sources near the ceiling region. It was originally thought that the scattered signal from dust particles and the Rayleigh scattered signal from air would saturate a CCD image. Regardless of these predictions, the camera successfully recorded a 3 cm diameter halo beam overflowing the 1.2 cm diameter upper baffle entrance hole area (Fig. 2), identifying this as a possible source of stray light. The CCD camera is specified to have a minimum detection threshold of 3.9×10^8 photons/cm². By making corrections for the camera lens collection efficiency and wavelength sensitivity at 1.06 μ m, as well as assumptions of the floor reflectivity and scattering distribution, we estimated the stray light level to be 5.1×10^4 photons/channel at the entrance to the collection lens.

Photons/channel at collection lens as measured by the camera =

$$A*B*C*D*E*F$$

- A = minimum detection threshold of camera at .54 μm =
 $3.9 \times 10^8 \text{ Photons/cm}^2$
- B = $1/(\text{collection enhancement from } \phi 2.5 \text{ cm, f/1.8 lens}) \ 1/(7.1) =$
0.13
- C = floor reflectivity = .3
- D = scattering distribution = $1 - \cos \phi$, where $\phi = 31^\circ$
- E = $1/(\text{relative CCD sensitivity at } 1.06 \mu\text{m vs. } 0.54 \mu\text{m}) =$
 $1/(0.1) = 10$
- F = collection efficiency of f/6.8 lens = area of lens/total scatter
area = $201 \text{ cm}^2 / [2 * \pi * (100 \text{ cm})^2] = 0.002154$

Given the CCD camera dynamic range of 1.5, the upper bound on the stray light level was 7.6×10^6 photons/channel, which is probably closer to the actual level because the image was near saturation. The estimated level at the lens as measured by the ADP detector was 6.3×10^6 photons/channel. This includes a correction factor of 0.008 for the combined transmission efficiency of the collection optics, fiber optics, and polychromatic filter box.

Photons/channel at collection lens as measured by APD detector =

$$A * B * C * D$$

- where: A = counts/ channel at detector = 50,000 counts
- B = $1/(\text{counts at detector/photons into polychromator box})$
= 0.015 counts/photon
- C = $1/(\text{transmission efficiency of fiber optic bundles}) =$
 $1/(0.59)$
- D = $1/(\text{transmission efficiency of collection optics and mirror}) = 1/(0.9)$

This good agreement between the camera and detector confirms that the halo beam imaged by the CCD camera was a major contributor to the stray light signal.

IV. BAFFLE MODIFICATIONS

To reduce the stray light generated from the halo beam at the ceiling, the upper baffle array apertures were enlarged to allow a more efficient propagation to the exit window and beam dump region. Use of the CCD camera was essential to determine the optimum aperture diameter. An oversized baffle could pass too much reflected light from the exit window, while an undersized baffle would be struck by the incoming halo beam. A larger 1 cm radial clearance was provided between the baffles and the halo beam as it expanded through the array (Fig. 1). However, with the larger baffles in place, the CCD camera was able to view further up into the exit baffle array and record saturated images of reflections from the exit window region. This stray light was reduced by tilting the exit window at Brewster's angle. A subsequent Rayleigh scattering measurement confirmed the enlarged baffles and new window significantly reduced the stray light level. It was now sufficiently low to allow a more accurate correlation of its time history relative to the Rayleigh signal. This enabled us to identify the exit window and beam dump region as the primary remaining source, rather than the exit baffles (Fig. 3)

Since the vessel was now evacuated for impending operations, the CCD camera was again used to survey the exit window region from outside the vessel. A significant reflection from the Brewster's window

was imaged, indicating that the laser polarization was not uniform as assumed. By installing a Glan-Laser polarizer before the focusing lens, the stray light was reduced by a factor of two, which was now sufficient to calibrate the upper eight channels (Fig. 4). Fortunately these channels had a constant density calibration factor which allowed us to extrapolate it to the remaining four channels whose stray light levels remained too large. Figure 5 illustrates how the upper eight channels view a floor region that is not directly illuminated with light from the exit window.

V. SOURCES OF STRAY LIGHT

We first postulated that the halo beam was actually diffracted light from either the circular input aperture in front of the focusing lens or the input baffles. However, with our aperture dimensions, the diffracted light level would be several orders of magnitude lower than the observed halo signal. It was also considered that the halo beam was generated by scatter off of the aperture in front of the focus lens since CCD camera images showed that up to 40% of the beam energy was being removed here to improve the its profile. Beam relay optics were installed between the laser output and the lens, which significantly improved the beam quality at the aperture location, but only had a minimal effect on the stray light level.

Although we were unsuccessful in identifying the stray light source at the time of initial system operation, subsequent bi-directional reflection distribution function measurements (BRDF) on the beam steering mirrors located below the vessel indicated they produced excessive scattered light levels.⁵ It was found that the hi-reflection coatings on these

mirrors were deposited at high temperatures in order to produce a more durable surface. This generates larger oxide grains within the coating material which scatter 10-15X more light than conventional coatings. Preliminary tests using only two of these low-scatter mirrors indicate that the stray light is reduced to acceptable levels on all channels.

ACKNOWLEDGMENTS

We wish to thank R. Ellis, D. Behne, G. Holtz, and G. Rolens for technical support, R. Wood for operations coordination, M.E. Fenstermacher and C Lasnier for video recording, J.C. DeBoo, R.D. Stambaugh, and S.L. Allen for program support. This work was supported by the U.S. Department of Energy under Contract No. DE-AC03-89ER51114 and W-7405-ENG-48.

a) Present address: General Atomics, P.O. Box 85608, San Diego,
California.

¹T.N. Carlstrom, et al., Rev. Sci. Instrum. **63**, 4901 (1992).

²T.N. Carlstrom, et al., Rev. Sci. Instrum. **66**, 493 (1994).

³D.G. Nilson, et al., (to be published in Fusion Engineering and Design)

⁴T.N. Carlstrom, et al., Rev. Sci. Instrum. (to be published)

⁵BRDF measurements performed by Schmitt Measurement Systems,
Portland, Oregon

Figure Captions:

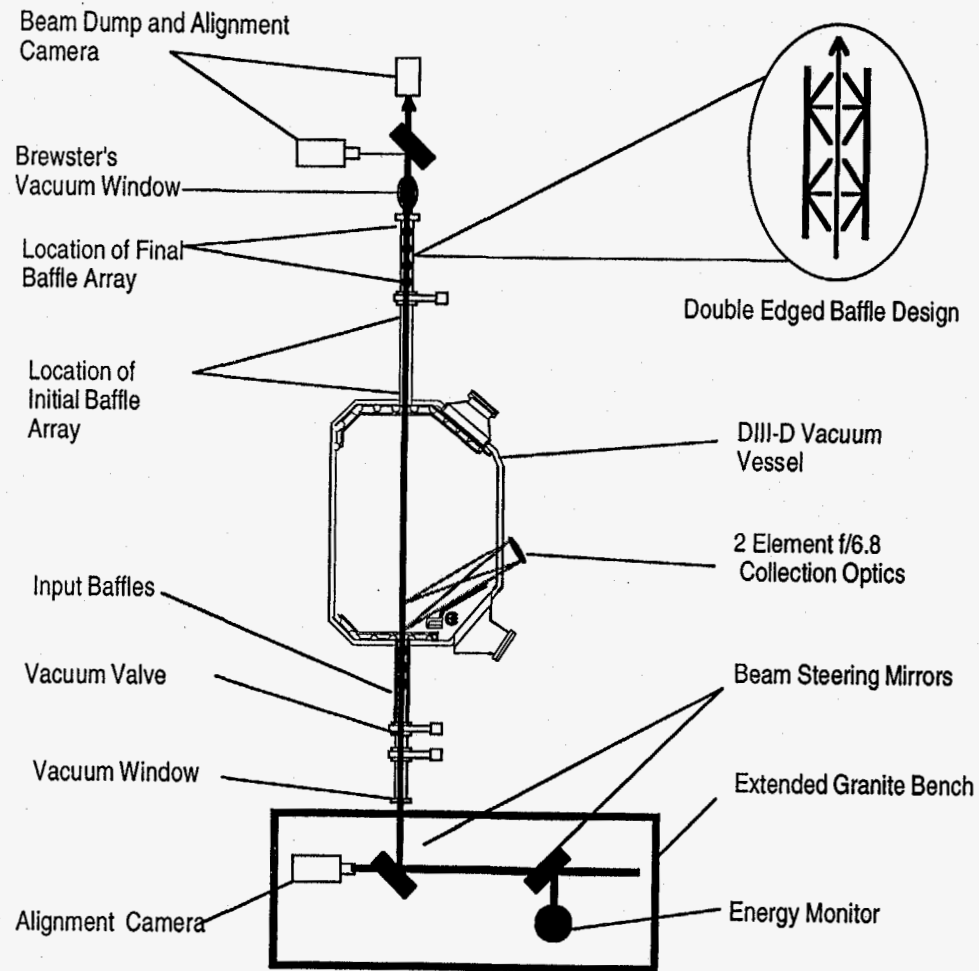
Fig. 1. The DIII-D divertor Thomson scattering systems uses baffle arrays in the entrance and exit ports to help eliminate stray laser light generated from the vacuum windows and laser input optics.

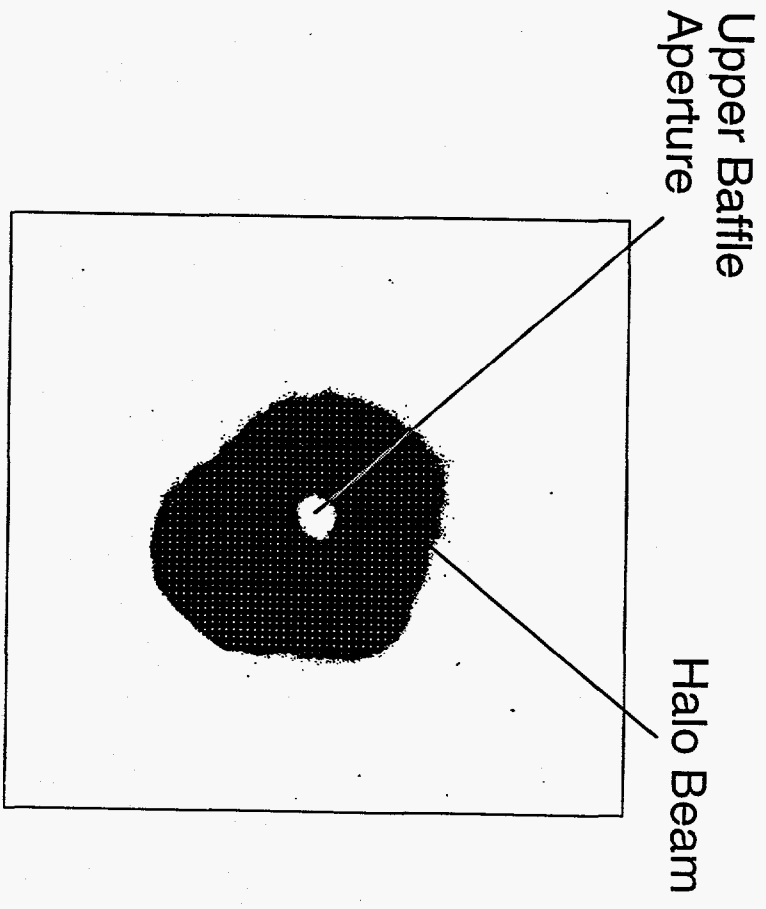
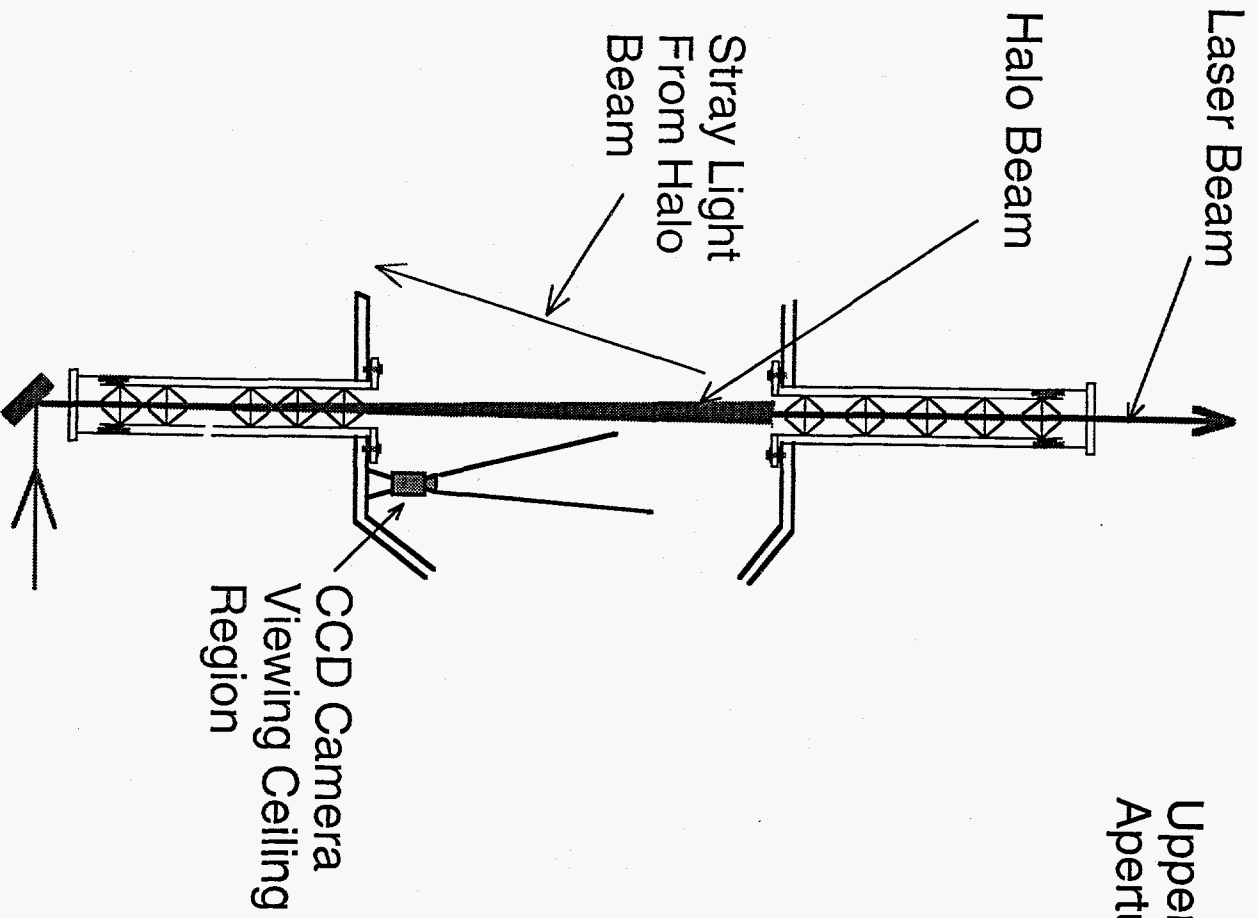
Fig. 2. A CCD camera placed on the vessel floor is able to image a halo beam striking the vessel ceiling. Photon level estimates from the images correlate well with the measured stray light level at the detector.

Fig. 3. When the stray laser light level is reduced to the same order as the Rayleigh scattered signal, its relative timing can then be used to locate the stray light source.

Fig. 4. By reducing the stray light level, a successful Rayleigh scattering calibration was obtained. This is indicated by the linear correlation between the scattered photons and the argon gas pressure.

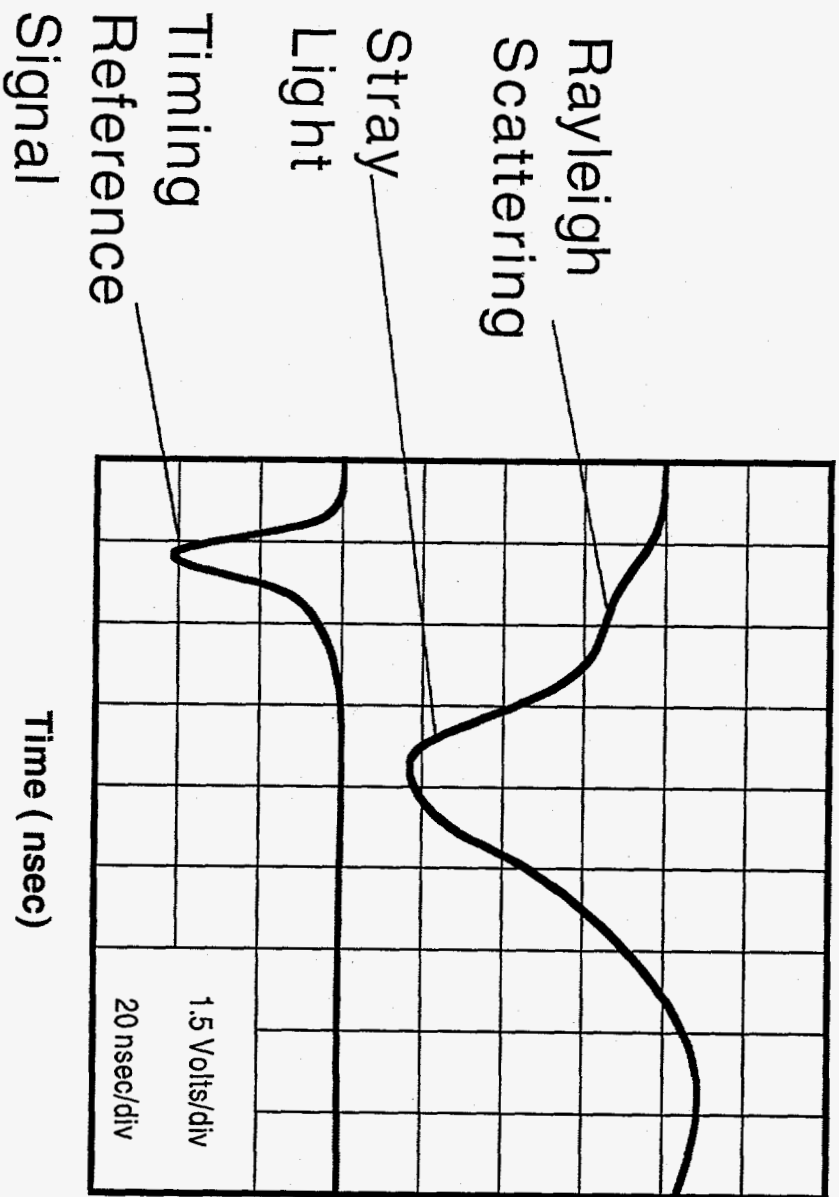
Fig. 5. The lower three viewing channels are saturated by the stray laser light originating from the upper exit window. The remaining nine channels do not have a direct view of this window, producing stray light levels low enough to achieve an accurate density calibration.



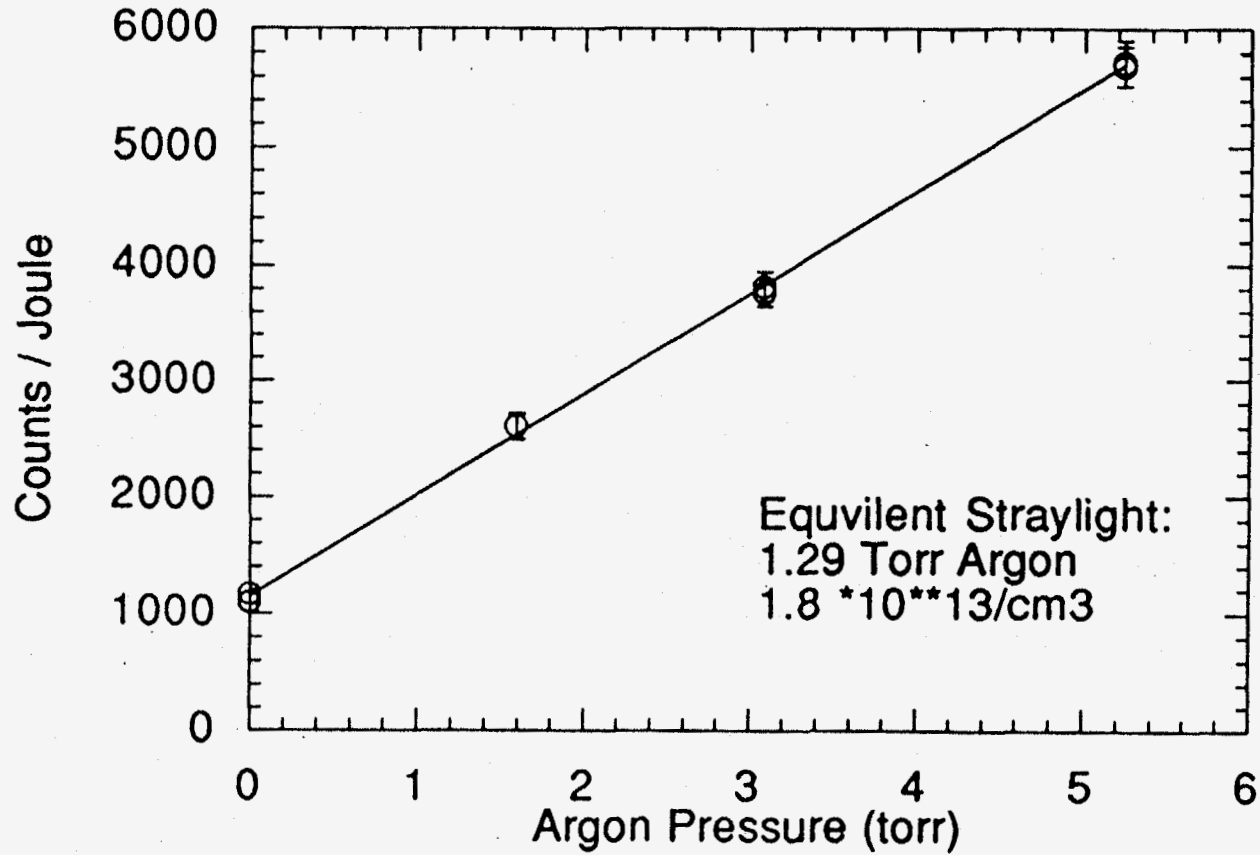


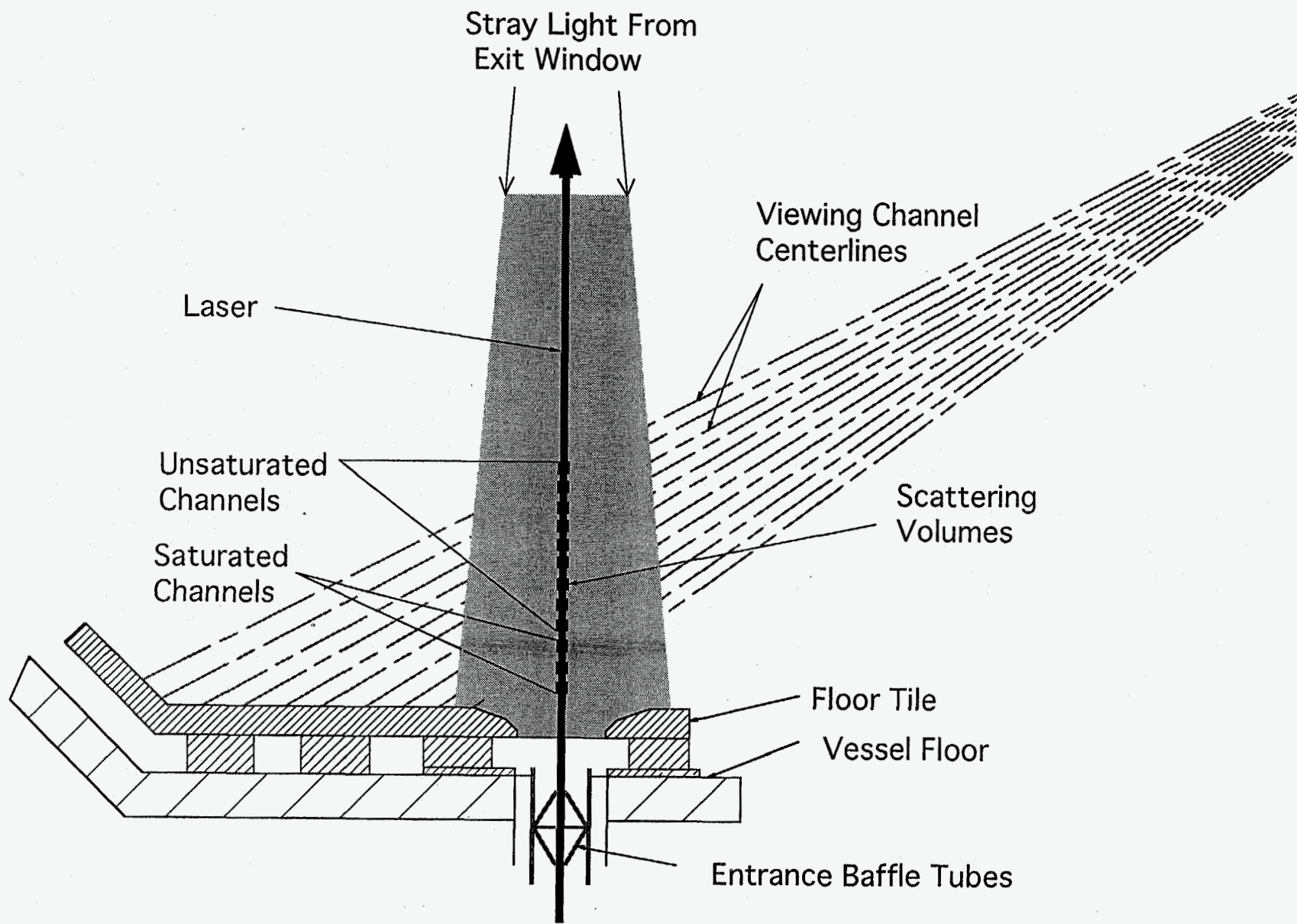
CCD Camera Image of Halo beam Striking Exit Baffles

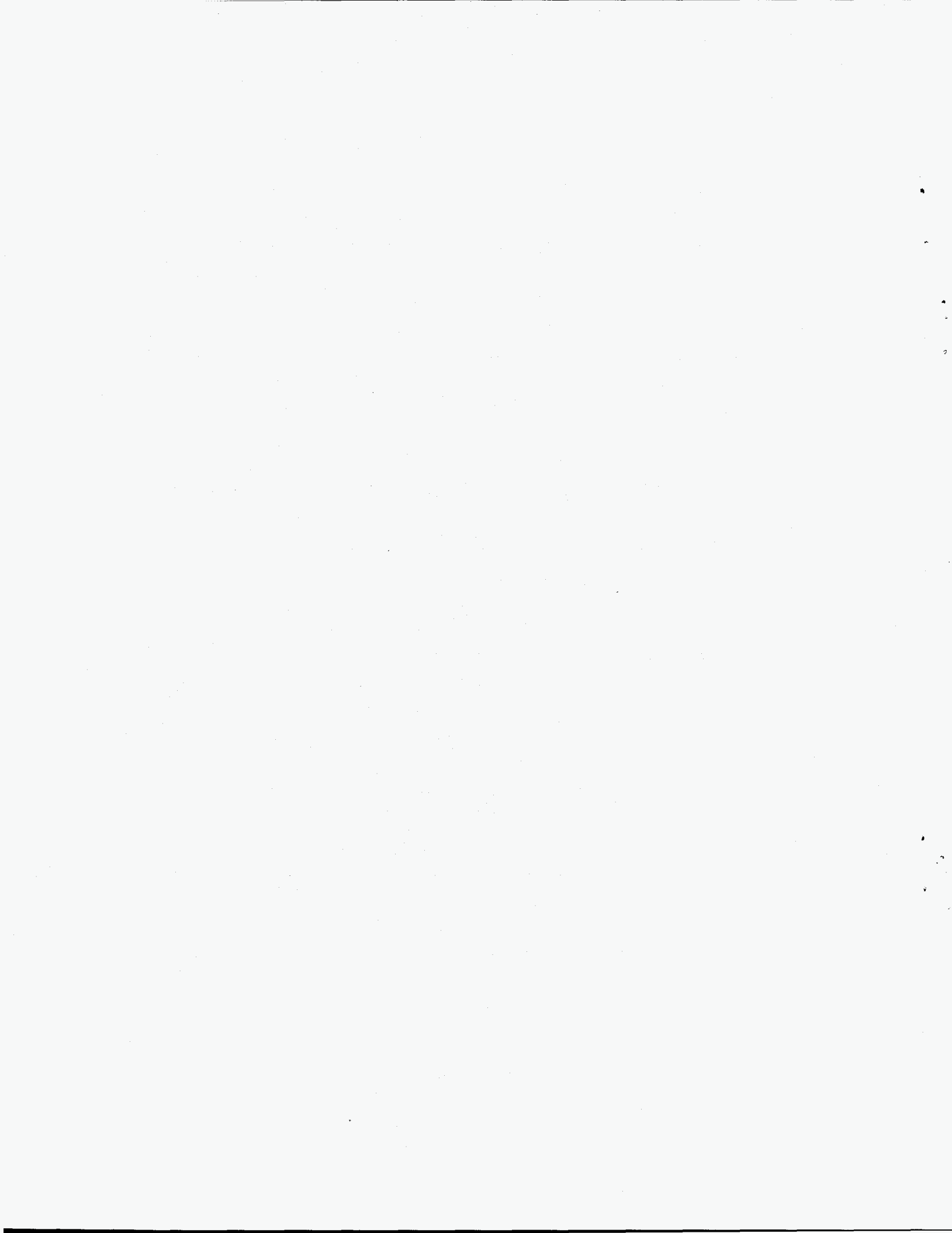
Channel 2, 65 ns digitizer

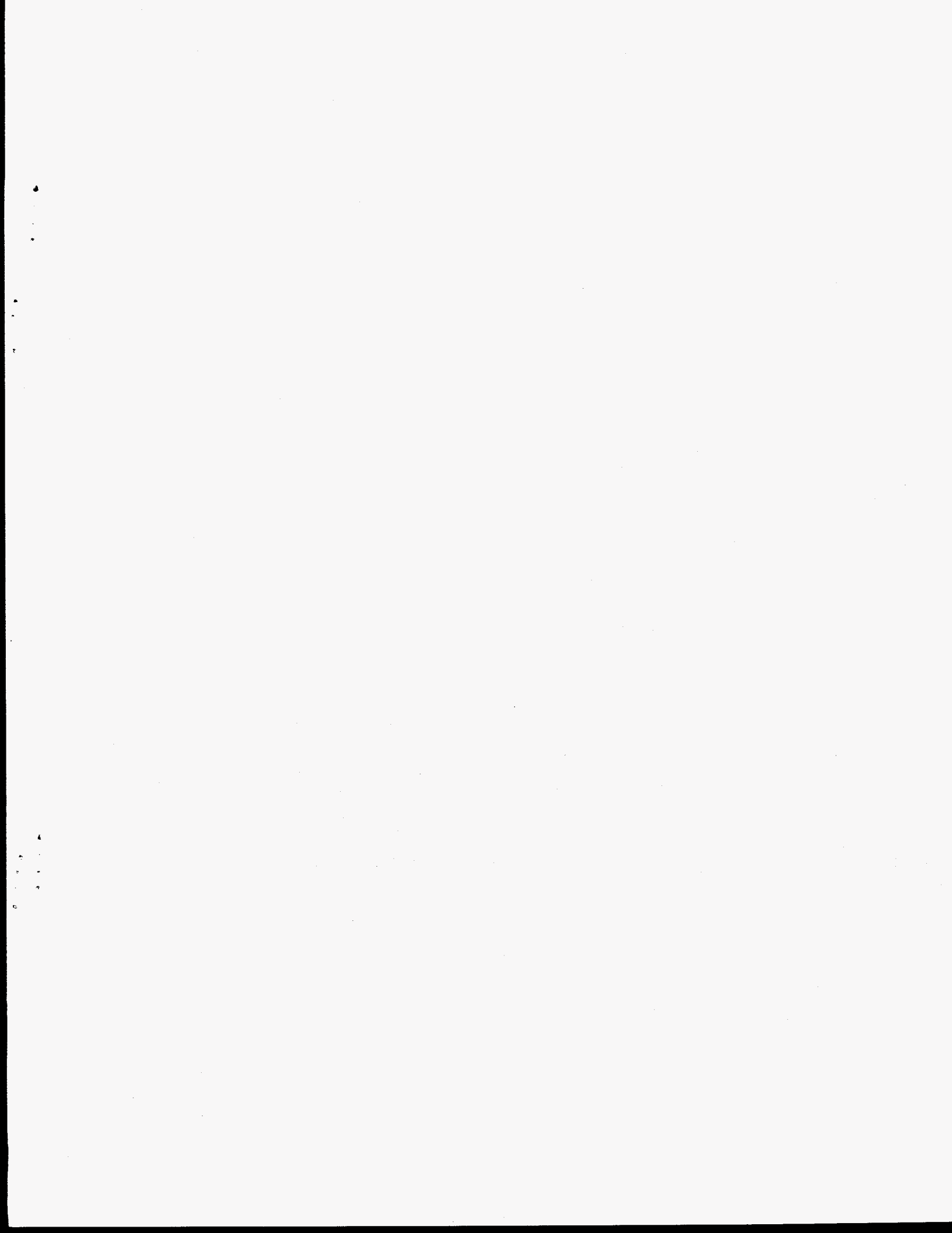


Divertor Thomson Rayleigh Signal, Channel 6









Technical Information Department • Lawrence Livermore National Laboratory
University of California • Livermore, California 94551

